CVJ CLUJ VETERINARY JOURNAL

*Article*

# Decoding the Glycan Signature of Hyalinized Pancreatic Carcinoma in Dogs: Histochemical and Lectin-Based Evidence of Extracellular Matrix Heterogeneity

**Ecaterina Semzenisi[1*], Corina Toma[1], Haralambie Mara[1], Dragoș Hodor[1], Romelia Pop[1], Sorana Cătoi[1], Ibrahima Mamadou Sall[1], Alexia-Teodora-Hoța[1], Alexandru Flaviu Tăbăran[1].**

[1] Department of Veterinary Pathology, Faculty of Veterinary Medicine, University of Agricultural Sciences and Veterinary Medicine, Cluj-Napoca, Romania
* Correspondence: ecaterina.semzenisi@student.usamvcluj.ro

**Abstract:** Hyalinizing pancreatic carcinoma in dogs is a rare tumor characterized by abundant eosinophilic extracellular material of uncertain composition. The aim of this study was to characterize the nature of hyaline deposits using histochemical and lectin-based methods. Pancreatic tissues from three dogs (two Boxers and one American Staffordshire Terrier) were examined following necropsy. Sections were stained with hematoxylin and eosin, Masson's Trichrome, and Congo Red, and analyzed using lectin histochemistry (SNA, PHA-L, ECL). All cases showed similar architecture, with neoplastic epithelial cells embedded in abundant hyaline stroma. Masson's Trichrome demonstrated collagen-rich deposits in all cases. Congo Red staining revealed heterogeneity, with negative staining in two cases and weak to transitional positivity in one case, interpreted as equivocal and not sufficient to confirm amyloid deposition. Lectin histochemistry showed variable glycosylation patterns among tumors. These findings indicate that hyaline in canine pancreatic carcinoma is not a uniform entity, but a heterogeneous extracellular material composed predominantly of collagen-rich stroma and glycoprotein-associated matrix, with inter-case biochemical variability. Combined histochemical and lectin-based approaches provide additional insight into the molecular complexity of these lesions.

**Keywords:** Hyalinizing pancreatic carcinoma, dog, lectin histochemistry, SNA, PHA-L, ECL, extracellular matrix, pancreas.

Received: 21.03.2026
Accepted: 03.06.2026
Published: 09.06.2026

*DOI:10.52331/v31i3xh43*



## 1. Introduction

The term *hyaline* was first used simply to describe extracellular material of uncertain nature that appeared glassy and eosinophilic on routine hematoxylin and eosin (H&E) sections. In the early decades of pathology, when special stains such as Congo Red were not yet widely available, this label served as a practical placeholder for deposits that looked similar but might have very different biological origins. As histopathology advanced, the concept of hyaline expanded to include a wide variety of smooth, homogeneous, pink-staining materials encountered in both neoplastic and non-neoplastic tissues. Early pancreatic studies had already noted hyaline in islet cell tumors [1], and mid-century investigations further complicated the picture by showing that some of these deposits behaved like amyloid in diabetic pancreases [2,3].

More recent work has shown that pancreatic hyaline is far from a uniform entity. In experimental rodent models, hyaline may accumulate within ductal epithelial cells [4], while in canine hyalinizing pancreatic adenocarcinoma, the deposits have been clearly demonstrated to be non-amyloid, lacking Congo Red positivity and immunoreactivity for amyloid A or islet amyloid polypeptide [5]. Together, these findings reveal that hyaline can represent a spectrum of extracellular products ranging from collagen-rich fibrotic stroma to glycoprotein-laden matrix material often arising from chronic inflammation, degeneration, or tumor-associated remodeling. Because many of these substances appear

deceptively similar on H&E, distinguishing between them requires targeted histochemical and immunohistochemical techniques.

Hyaline material has also been reported in a number of human pancreatic tumors, including solid pseudopapillary neoplasms (SPNs), intraductal papillary mucinous neoplasms (IPMNs), and ductal adenocarcinomas. In these contexts, it often appears as intracytoplasmic or stromal globules that are PAS-positive and diastase-resistant [6,7]. Hyalinizing changes may also accompany exocrine neoplastic or metaplastic processes [8] and can occasionally be seen in endocrine tumors or syndromic conditions such as MEN.

Given that many forms of hyaline contain glycoproteins or other carbohydrate-rich molecules, lectin histochemistry offers an attractive strategy for deeper biochemical characterization. Lectins bind selectively to defined glycan motifs and have been widely used to characterize glycosylation patterns in pancreatic tissues, including acinar cells and neoplastic lesions [9–11]. In pancreatic cancer models, lectin binding studies have demonstrated tumor-specific glycosylation patterns associated with malignant transformation [12–14]. Lectins such as Sambucus nigra agglutinin (SNA), Phaseolus vulgaris leucoagglutinin (PHA-L), and Erythrina cristagalli lectin (ECL) are particularly informative because they map specific glycan signatures respectively, $\alpha$2,6-linked sialic acids, complex branched N-glycans, and galactose-containing residues [15,16]

Although hyalinizing pancreatic carcinoma has been reported in dogs [5], the biochemical nature of the hyaline material in these tumors remains poorly defined. To date, no study has applied lectin histochemistry to investigate the glycan composition of hyalinized stroma in canine pancreatic neoplasms.

The aim of this study was to characterize the glycosylation profile and biochemical nature of hyaline material in three canine pancreatic carcinomas using lectin histochemistry and histochemical stains, and to determine whether these deposits represent collagenous or glycoprotein-rich extracellular components and to assess whether any cases show Congo Red reactivity suggestive of proteinaceous extracellular component.

## 2. Materials and Methods

### *2.1. Case Selection*

Pancreatic tissue samples were obtained from three dogs: a 10-year-old male Boxer (Case 1), a 12-year-old American Staffordshire Terrier (Case 2), and a 12-year-old female Boxer (Case 3). All animals were diagnosed with pancreatic neoplasia during routine diagnostic necropsy performed at the Department of Pathology, University of Agricultural Sciences and Veterinary Medicine (USAMV), Cluj-Napoca, Romania.

### *2.2. Ethical Approval*

The study was conducted in accordance with national and European regulations on animal research and was approved by the Bioethics Committee of the University of Agricultural Sciences and Veterinary Medicine (USAMV) Cluj-Napoca, Romania, under Ethical Approval Decision corresponding to Application Form No. 513/29.09.2025

### *2.3.Necropsy, Sample Collection, and Tissue Preparation*

Necropsies were carried out following standard anatomical and pathological dissection protocols. Pancreatic lesions were identified macroscopically, excised together with adjacent parenchyma, and immediately immersed in 10% neutral-buffered formalin for fixation. Given the minute size and complex cellular architecture of neuroendocrine structures examined in related cases, meticulous handling was required to preserve tissue integrity. Fixed samples were processed routinely, dehydrated through graded ethanol (80%, 95%, 100%), cleared in xylene, and embedded in paraffin. Serial sections of 2–3 μm thickness were obtained using a rotary microtome and mounted on charged slides.

### *2.4.Histology and Special Stains*

Routine histological examination was performed on hematoxylin and eosin (H&E) stained sections. To further characterize the extracellular matrix and the hyaline stromal component Masson's Trichrome staining was performed to evaluate collagen deposition and stromal fibrosis using a standard protocol with hematoxylin, Biebrich scarlet–acid fuchsin, and aniline blue [17].

Congo Red staining was performed to evaluate the affinity of extracellular material for Congo Red and to differentiate Congo Red-reactive deposits from other eosinophilic extracellular materials. Sections were stained following a Highman-based protocol with alkaline differentiation and evaluated under bright-field microscopy [18,19].

*2.5.Lectin Histochemistry*

Lectin histochemistry was employed to investigate the glycosylation patterns of tumor cells and hyalinized stroma, based on the established utility of lectins in mapping carbohydrate structures and identifying glycoprotein-rich secretory zones in endocrine and neuroendocrine tissues (Shimomura, 2018; Syed, 2016). Paraffin sections were deparaffinized in xylene, rehydrated through descending alcohols, and rinsed in distilled water. Slides were then incubated for 60 minutes at room temperature with a panel of fluorescein-labeled lectins, each targeting specific glycan motifs:

Sambucus nigra agglutinin (SNA): $\alpha$2,6-linked sialic acid

Phaseolus vulgaris leucoagglutinin (PHA-L): β1,6-branched complex N-glycans

Erythrina cristagalli lectin (ECL): Galβ1-4GlcNAc residues

Following lectin incubation, slides were washed twice in distilled water and counterstained with Draq5 (5 minutes) to highlight nuclei. All staining procedures were performed exactly according to the manufacturer's recommendations and previously validated protocols [20].

*2.6. Confocal Microscopy and Image Acquisition*

Fluorescent lectin binding was evaluated using a Zeiss LSM 710 laser-scanning confocal microscope mounted on an Axio Observer Z1 inverted platform. Image acquisition parameters were as follows: Excitation: 543 nm for Rhodamine-labeled lectins (emission BP 548–629 nm) and 633 nm for Draq5 (emission BP 661–759 nm) Objective: Plan-Apochromat 63×/1.4 NA oil immersion (DIC 27). Beam splitter: MBS 488/543/633. Images were captured, processed, and analyzed using ZEN software (Zeiss). Fluorescence intensity values were expressed as arbitrary units (AU), following established quantification protocols for lectin-based confocal analysis [13].

*2.7. Lectin Binding Evaluation*

Lectin reactivity was assessed semi-quantitatively by two independent observers, using the following scoring system: 0: no labeling +: weak labeling ++: moderate labeling +++: strong labeling Discrepancies were resolved by consensus assessment during joint slide review sessions.

**Table 1.** Lectins used in the study and their binding specificities

| Lectin | Binding specificity | Application | Reference |
|---|---|---|---|
| Sambucus nigra agglutinin (SNA) | $\alpha$2,6-linked sialic acid residues | Detection of increased sialylation in pancreatic neoplasia | Wagatsuma et al., 2020; Holst et al., 2017 |
| Phaseolus vulgaris leucoagglutinin (PHA-L) | β1,6-branched complex N-glycans | Identification of altered N-glycan branching in tumors and fibrotic tissue | Wagatsuma et al., 2020; McDowell et al., 2021 |
| Erythrina cristagalli lectin (ECL) | Galβ1-4GlcNAc residues | Detection of galactose-containing glycans in inflammation and neoplasia | Wagatsuma et al., 2020; McDowell et al., 2021 |

**3. Results**

*3.1. Histopathology*

Three cases of hyalinizing pancreatic carcinoma were examined, and the main findings are presented below, including histopathological features, special stains, and lectin-binding profiles.

Histologically, the neoplasms were unencapsulated and infiltrative, consisting of neoplastic epithelial cells arranged predominantly in irregular tubular, acinar, and tubulocystic structures supported by a fibrovascular stroma. Neoplastic cells were cuboidal to columnar, with moderate to abundant eosinophilic cytoplasm containing fine apical granules and round to oval basally located nuclei with coarsely stippled chromatin and prominent nucleoli. Mild to moderate anisocytosis and anisokaryosis were observed.

A prominent hyalinized collagenous stroma surrounded and separated the neoplastic glands, forming broad eosinophilic extracellular deposits. Multifocally, the hyalinized material expanded the interstitial

stroma and accumulated within glandular lumina. The neoplastic proliferation exhibited an infiltrative growth pattern, extending into the adjacent pancreatic parenchyma and surrounding connective tissues.

Mitotic activity was low, with 3 mitotic figures per 2.37 mm² in Cases 1 and 2 and 5 mitotic figures per 2.37 mm² in Case 3. Occasional intraluminal accumulations of cellular debris and rare inflammatory cells were observed. Tumor necrosis was absent in all cases. The stromal inflammatory response was minimal and consisted of scattered lymphocytes and macrophages.

Vascular invasion was identified in Case 3, characterized by aggregates of neoplastic epithelial cells within endothelial-lined vascular spaces. Omental metastases were also present in Case 3. No vascular invasion or metastatic lesions were identified in Cases 1 and 2. Overall, the tumors were well differentiated and exhibited features consistent with hyalinizing pancreatic adenocarcinoma (Fig. 1A-I).

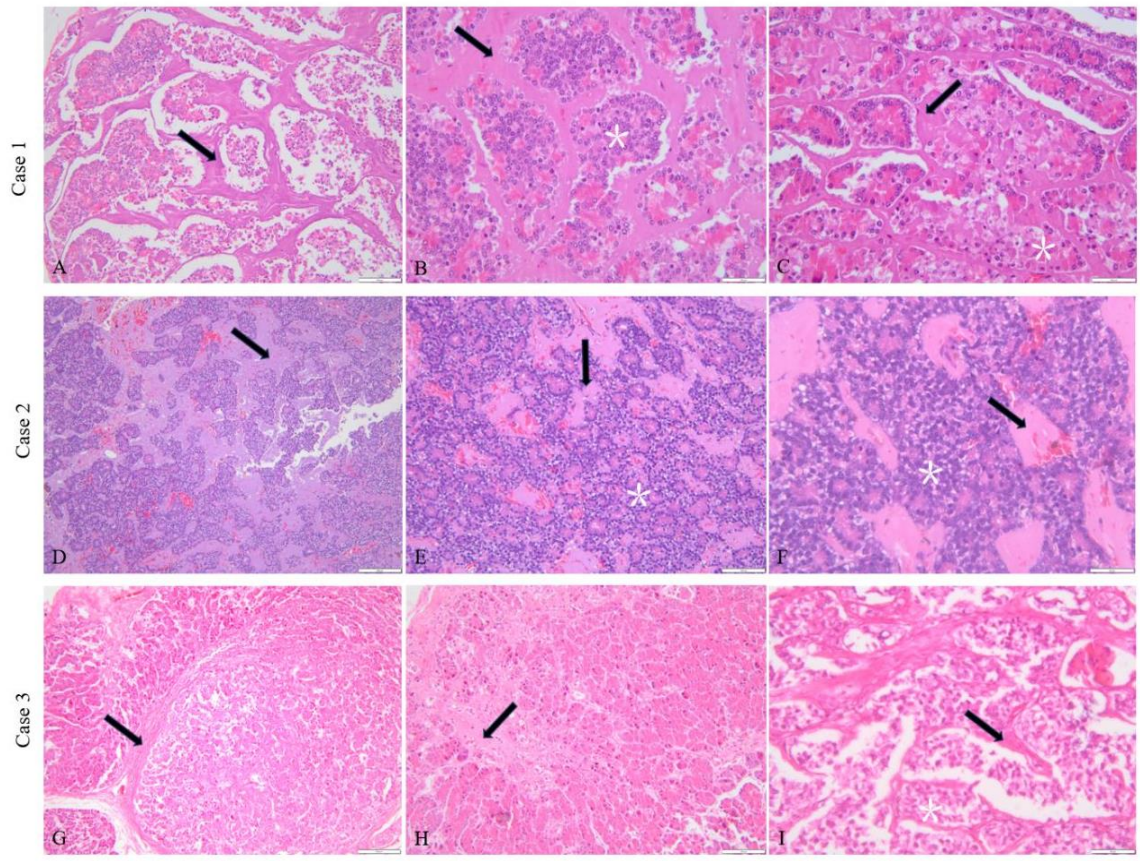


**Figure 1. Pancreatic adenocarcinoma.** (A–C) Neoplastic cells predominantly arranged in acinar structures (*asterisks*), separated by abundant eosinophilic, homogeneous hyaline stroma (arrows). (A) 20×, scale bar = 200 μm. (B) 10×, scale bar = 50 μm. (C) 20×, scale bar = 50 μm.

### *3.2. Histochemical characterization of hyaline material*

#### 3.2.1. Masson's Trichrome staining

In all three cases, Masson's Trichrome strongly highlighted the hyaline material as collagen-rich pale blue stromal deposits separating nests of tumor cells. Fine collagen septa extended between tumor islands, confirming the collagenous nature of the stroma (Fig. 2A–C).

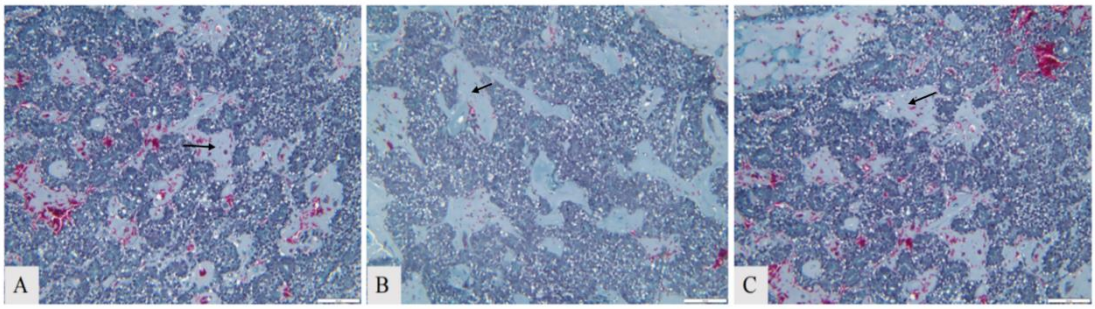


**Figure 2. Histological appearance of hyalinizing pancreatic carcinoma using Masson's Trichrome staining. Cases 1–3 (A–C).** The hyaline stroma is highlighted as broad pale blue collagen-rich deposits (arrow) separating nests of tumor cells. Fine collagen septa extend between tumor islands, confirming the collagenous nature of the stroma. Scale bar: 50 μm.

3.2.2. Congo Red staining

Congo Red staining revealed heterogeneity among cases. Two cases were negative, whereas one case showed weak to transitional Congo Red reactivity within the hyaline material (Fig. 3A–C). Because polarized light examination and additional confirmatory analyses were not performed, the findings were considered equivocal and insufficient to confirm amyloid deposition.

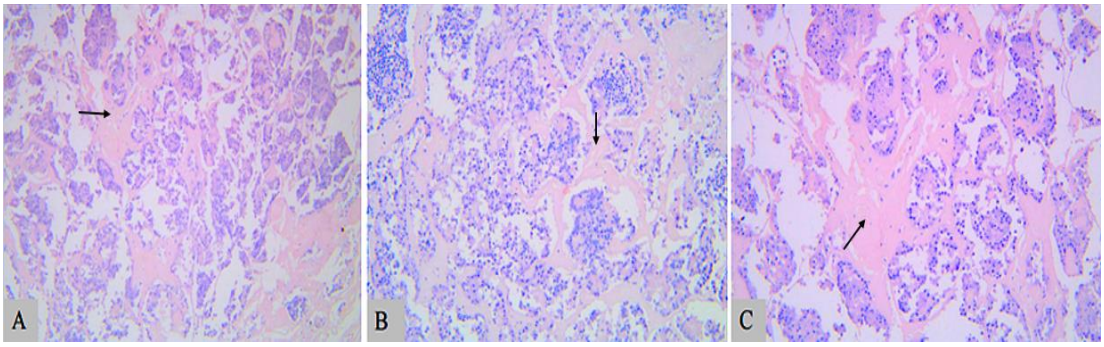


**Figure 3. Histological appearance of hyalinizing pancreatic carcinoma using Congo Red staining.** Case 2 (A–C). Arrows indicate areas of weak to transitional Congo Red reactivity within homogeneous eosinophilic hyaline deposits located in the tumor stroma. Because polarized light examination and confirmatory analyses were not performed, the findings were considered equivocal and not diagnostic of amyloid deposition. Cases 1 and 3 were negative (not shown). Scale bar: 50 μm.

*3.3. Lectin histochemistry*

In Cases 1 and 2, SNA and ECL labeling was observed predominantly within the extracellular hyalinized stromal matrix (indicated by white asterisks), whereas only limited staining was present in neoplastic epithelial cells. In contrast, Case 3 exhibited predominantly cytoplasmic and membranous SNA labeling of neoplastic cells. PHA-L reactivity was localized mainly within the cytoplasm of neoplastic epithelial cells, being strongest in Cases 1 (Fig. 5) and 3 and weak in Case 2. No specific nuclear lectin labeling was observed; blue fluorescence corresponds to DRAQ5 nuclear counterstaining (Fig. 4A–C).

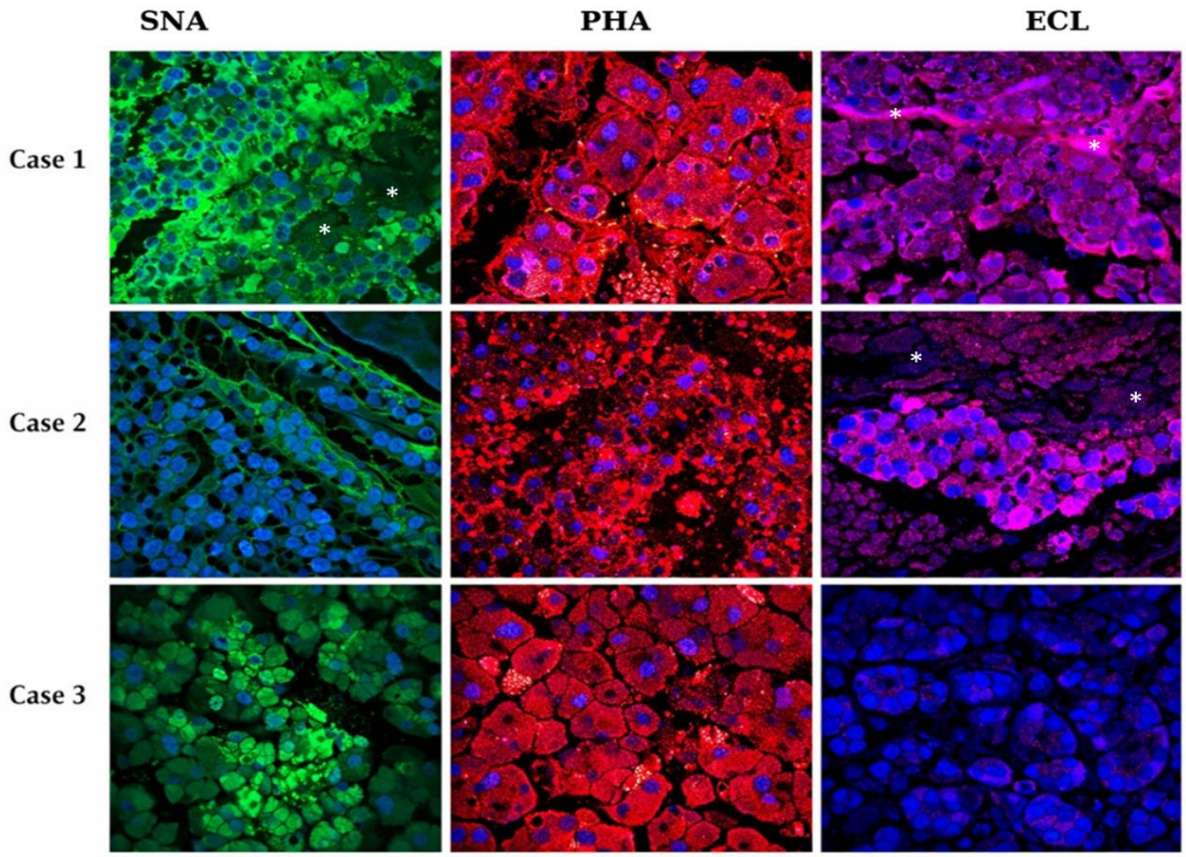


**Figure 4. Lectin histochemical staining patterns in hyalinizing pancreatic carcinoma. Cases 1–3 (A–C).** White asterisks indicate the hyalinized stromal matrix. Blue fluorescence corresponds to DRAQ5 nuclear counterstaining. In Case 1, strong SNA (+++) reactivity was observed predominantly within the hyalinized stromal matrix, while PHA-L showed moderate to strong cytoplasmic labeling of neoplastic epithelial cells and ECL demonstrated weak reactivity. Case 2 exhibited weak SNA labeling and weak cytoplasmic PHA-L (+) reactivity in neoplastic epithelial cells. In Case 3, moderate SNA (++) labeling was observed, accompanied by strong cytoplasmic and membranous PHA-L reactivity, whereas ECL labeling was absent or minimal. No consistent lectin labeling was observed within vascular structures or necrotic areas. These findings indicate variability in lectin-binding patterns and extracellular matrix heterogeneity among cases.

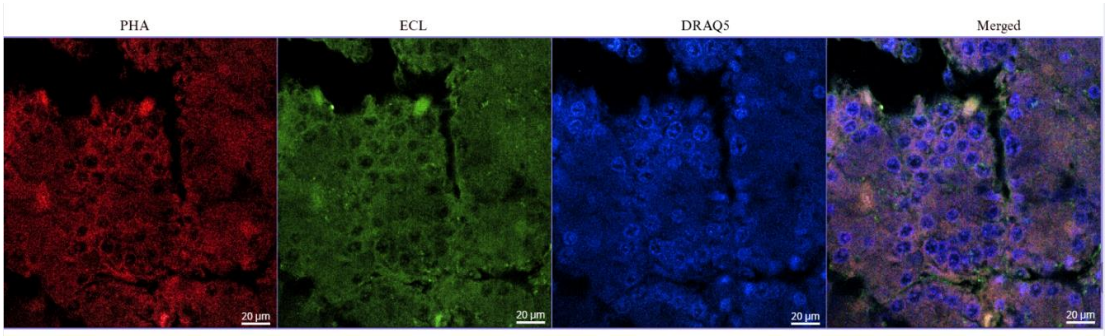


**Figure 5. Representative confocal image of hyalinizing pancreatic carcinoma (Case 1)** stained with *Phaseolus vulgaris leucoagglutinin* (PHA-L; red) and *Erythrina cristagalli* lectin (ECL; green). DRAQ5 (blue) was used as a nuclear counterstain. PHA-L showed strong diffuse cytoplasmic and membranous labeling of neoplastic epithelial cells, while ECL exhibited weaker diffuse cytoplasmic staining. The merged image highlights the distribution of lectin-reactive glycoconjugates within the tumor cell population. Scale bar = 20 µm.

## 4. Discussion

The findings of this study indicate that hyaline material in canine pancreatic carcinoma should not be viewed as a single, uniform structure. Although it appears similar under routine histological examination, its composition varies between cases. In all tumors examined, Masson's Trichrome staining demonstrated a strong collagen component, supporting the idea that hyalinization is largely driven by extracellular matrix remodeling and collagen deposition within the tumor microenvironment.

At the same time, Congo Red staining revealed a different layer of complexity. Two cases showed no reactivity, whereas one case displayed weak to transitional positivity within the hyaline areas. This result suggests that, in some instances, the stromal material may include an additional proteinaceous component with affinity for Congo Red. However, the staining intensity and distribution were limited, and therefore insufficient to support a definitive diagnosis of amyloid. In this context, the observed reactivity should be interpreted cautiously and considered suggestive rather than conclusive. These observations are generally in agreement with previous reports describing hyaline stroma in canine pancreatic tumors as predominantly non-amyloid [5]. The presence of weak Congo Red reactivity in one case, however, raises the possibility that the biochemical composition of this material may be more variable than previously assumed. Such variability could be related to differences in tumor biology, local microenvironmental conditions, or the dynamic nature of extracellular matrix production and modification. It may also reflect technical and interpretative factors inherent to histochemical staining. The mechanisms underlying hyaline formation in these tumors are likely multifactorial [21]. The consistent presence of collagen supports the role of stromal activation and fibroblast-driven matrix production. In contrast, the case showing partial Congo Red reactivity may represent either a distinct form of extracellular protein accumulation or a modification of existing matrix components. It is also possible that the staining reflects structural or chemical alterations in the matrix rather than true amyloid deposition. Without confirmatory methods such as polarized light examination or immunohistochemical characterization, this distinction cannot be definitively made [22].

Additional insight was provided by lectin histochemistry, which revealed differences in glycosylation patterns among the cases. Variations in SNA, PHA-L, and ECL binding indicate that the carbohydrate composition of the extracellular matrix is not consistent across tumors. These differences suggest that even when hyaline material appears morphologically similar, these differences may reflect variation in lectin binding patterns and extracellular matrix composition among cases. Interestingly, the case with weak Congo Red reactivity also showed a distinct lectin-binding profile, further supporting the idea of biochemical heterogeneity [12].

Taken together, these findings highlight the importance of using multiple complementary techniques when evaluating extracellular material in neoplastic tissues. While standard histochemical stains provide valuable structural information, lectin histochemistry offers additional insight into molecular composition. The combined approach used in this study underscores that hyaline material in canine pancreatic carcinoma represents a spectrum of extracellular matrix alterations rather than a single defined entity.

This study is not without limitations. The relatively small number of cases limits the extent to which these findings can be generalized. In addition, the nature of the Congo Red-reactive material in one case remains uncertain, as no confirmatory analyses were performed. Future investigations involving larger case series and additional diagnostic methods will be necessary to better define the composition and biological significance of hyaline material in these tumors. Additional limitations include the absence of polarized light evaluation and the lack of normal or adjacent non-neoplastic pancreatic tissue for comparative lectin analysis. Therefore, Congo Red reactivity and lectin binding patterns should be interpreted descriptively and cannot be considered diagnostic of amyloid deposition or tumor-specific glycosylation.

## 5. Conclusions

In summary, the results of this study show that hyaline material in canine pancreatic carcinoma is heterogeneous in nature and cannot be considered a single, uniform structure. Collagen deposition, as demonstrated by Masson's Trichrome staining, was a consistent feature in all cases and appears to play a central role in the formation of this material.

Congo Red staining further highlighted variability between tumors, with two cases showing no reactivity and one case exhibiting weak to transitional positivity. Although this finding may suggest the presence of an additional protein component with Congo Red affinity, it does not provide sufficient evidence to confirm amyloid deposition.

Lectin histochemistry demonstrated variation in lectin binding among cases, supporting extracellular matrix heterogeneity.

Overall, this study emphasizes the value of combining histochemical and lectin-based methods to achieve a more nuanced understanding of extracellular matrix changes in canine pancreatic carcinoma. Further research, including confirmatory techniques, will be essential to clarify the nature of Congo Red-reactive material and to better understand the mechanisms underlying hyaline formation in these tumors.

**Author Contributions:** Conceptualization, E.S. and A.F.T.; methodology, E.S., C.T. and H.M.; software, E.S.; validation, E.S., C.T. and S.C.; formal analysis, E.S. and A.F.T.; investigation, E.S., C.T., H.M. and H.D.; resources, A.F.T., R.P. and S.C.; data curation, E.S.; writing—original draft preparation, E.S.; writing—review and editing, A.F.T., C.T. and S.C.; visualization, E.S. and A.-T.H.; supervision, A.F.T.; project administration, A.F.T.; funding acquisition, A.F.T. All authors have read and agreed to the published version of the manuscript.

**Funding:** This study was supported by the University of Agricultural Sciences and Veterinary Medicine, Cluj-Napoca.

**Institutional Review Board Statement:** Not Applicable

**Acknowledgments:** The authors gratefully acknowledge the technical staff of the Department of Veterinary Pathology, University of Agricultural Sciences and Veterinary Medicine, Cluj-Napoca, for their valuable assistance with tissue processing, histological staining, and laboratory procedures. The authors also thank the personnel involved in confocal microscopy and imaging support.

**Conflicts of Interest:** The authors declare no conflict of interest.

## References

1. Laidlaw, G.F. Nesidioblastoma, the islet tumor of the pancreas. *Am J Pathol* **1938**, *14*, 125–134.
2. Ahronheim, J. The nature of the hyaline material in the pancreatic islands in diabetes mellitus. *Am J Pathol* **1943**, 19, 873–880.
3. Warren, S.; LeCompte; P.M. *The pathology of diabetes mellitus*. 3rd ed: Lea & Febiger, Philadelphia, 1952.
4. Nolte, T.; Brander-Weber, P.; Dangler, C.; Deschl, U.; Elwell, M.R.; Greaves, P.; et al. Nonproliferative and proliferative lesions of the gastrointestinal tract, pancreas and salivary glands of the rat and mouse. *J Toxicol Pathol* **2016**, *29*(Suppl), 1S–125S.
5. Dennis, M.M.; O'Brien, T.D.; Wayne, T.; Kiupel, M.; Williams, M.; Powers, B.E. Hyalinizing pancreatic adenocarcinoma in six dogs. *Vet Pathol* **2008**, *45*, 475–483.
6. Samad, A.; Shah, A.A.; Stelow, E.B.; Alsharif, M.; Cameron, S.E.H.; Pambuccian, S.E. Cercariform cells: another cytologic feature distinguishing solid pseudopapillary neoplasms from pancreatic endocrine neoplasms and acinar cell carcinomas in endoscopic ultrasound-guided fine-needle aspirates. *Cancer Cytopathol* **2013**, *121*, 298–310.
7. Bhatnagar, R.; Olson, M.T.; Fishman, E.K.; Hruban, R.H.; Lennon, A.M.; Ali, S.Z. Solid-pseudopapillary neoplasm of the pancreas: cytomorphologic findings and literature review. *Acta Cytol* **2014**, *58*, 347–355.
8. Stanger, B.Z.; Stiles, B.; Lauwers, G.Y.; Bardeesy, N.; Mendoza, M.; Wang, Y.; et al. Pten constrains centroacinar cell expansion and malignant transformation in the pancreas. *Cancer Cell* **2000**, *8*, 185–195.
9. Shimomura, O.; Oda, T.; Tateno, H.; Ozawa, Y.; Kimura, S.; Sakashita, S.; et al. A novel therapeutic strategy for pancreatic cancer: targeting cell surface glycan using rBC2LC-N lectin-drug conjugate (LDC). *Mol Cancer Ther* **2018**, *17*, 183–195.
10. Syed, P.; Gidwani, K.; Kekki, H.; Leivo, J.; Pettersson, K.; Lamminmäki, U. Role of lectin microarrays in cancer diagnosis. *Proteomics*. **2016**, *16*, 1257–1265.
11. Jonas, L.; Fulda, G.; Walzel, H.; Schulz, U. Lectin binding studies with FITC-marked WGA and UEA I and flow-cytometric measurements on isolated rat pancreatic acinar cells. *Acta Histochem* **1993**, *95*, 45–52.
12. Wagatsuma, T.; Nagai-Okatani, C.; Matsuda, A.; Masugi, Y.; Imaoka, M.; Yamazaki, K.; et al. Discovery of pancreatic ductal adenocarcinoma-related aberrant glycosylations: a multilateral approach of lectin microarray-based tissue glycomic profiling with public transcriptomic datasets. *Front Oncol* **2020**, *10*, 338.
13. McDowell, C.T.; Klamer, Z.; Hall. J.; West, C.A.; Wisniewski, L.; Powers, T.W.; Angel, P.M.; Mehta, A.S.; Lewin D.N.; Haab, B.B.; Drake, R.R. Imaging mass spectrometry and lectin analysis of N-linked glycans in carbohydrate antigen-defined pancreatic cancer tissues. *Mol Cell Proteomics* **2021**, *20*, 100012.
14. Nishimura, N.; Saito, S.; Kubota, Y.; Moto-o, N.; Taguchi, K.; Yamazaki, K.; et al. Newly established human pancreatic carcinoma cell lines and their lectin binding properties. *Int J Pancreatol* **1993**, *13*, 31–41.
15. Xiao, X.; Fischbach, S.; Fusco, J.; Zimmerman, R.; Song, Z.; Nebres, P.; et al. PNA lectin for purifying mouse acinar cells from the inflamed pancreas. *Sci Rep* **2016**, *6*, 21127.
16. Holst. S.; Belo, A.I.; Giovannetti, E.; Van Die, I.; Wuhrer, M. Profiling of different pancreatic cancer cells used as models for metastatic behaviour shows large variation in their N-glycosylation. *Sci Rep* **2017,** *7*, 16623.
17. Bancroft, J.D.; Gamble, M. *Theory and practice of histological techniques*. 6th ed.; Churchill Livingstone Elsevier; Philadelphia, 2008.
18. Highman, B. Improved methods for demonstrating amyloid in paraffin sections. *Arch Pathol* **1946**, *41*, 559–562.
19. Yakupova, E.I.; Bobyleva, L.G.; Vikhlyantsev, I.M.; Bobylev, A.G. Congo Red and amyloids: history and relationship. *Biosci Rep* **2019**, *39*, BSR20181415.

20. Rebelo, A.L.; Contessotto, P.; Joyce, K.; Kilcoyne, M.; Pandit, A. An optimized protocol for combined fluorescent lectin/immunohistochemistry to characterize tissue-specific glycan distribution in human or rodent tissues. STAR Protoc **2021**, *2*, 100237.
21. Shiratori, S.; Sugiura, R.; Kuwatani, M.; Oda, S.; Nozawa, S.; Yonemura, H.; et al. Rare pancreatic neuroendocrine tumor with hyalinization exhibiting atypical imaging features: a case report. *Pancreas* **2025**, *54*, e499–e501.
22. Shashi, A.; Sharma, N.; Bhardwaj, M. Pathological evaluation of pancreatic exocrine glands in experimental fluorosis. *Asian Pac J Trop Med* **2010**, *3*, 36–40.